International Journal of Biochemistry Research & Review
5(1): 27-38, 2015, Article no.IJBcRR.2015.004
ISSN: 2231-086X

SCIENCEDOMAIN *international*
www.sciencedomain.org

In Silico Inhibitory Activity against Caspase 3 by Zinc (II) Coordinated Complexes

Nura Suleiman Gwaram[1,2*] and Pouya Hassandarvish[3]

[1]Chemistry Department, Faculty of Science, University of Malaya, 50603 Kuala Lumpur, Malaysia.
[2]Chemistry Department, Faculty of Natural and Applied Sciences, Umaru Musa Yar'adua University, P .M.B. 2218 Katsina, Nigeria.
[3]Molecular Medicine Department, Faculty of Medicine, University of Malaya, 50603 Kuala Lumpur, Malaysia.

Authors' contributions

This work was carried out in collaboration between both authors. Author NSG designed the study, performed the synthesis of the complexes and molecular docking experiments and wrote the first draft of the manuscript. Author PH performed the antioxidant testing of the compounds. Both authors read and approved the final manuscript.

Article Information

DOI: 10.9734/IJBcRR/2015/12979
Editor(s):
(1) Carmen Lúcia de Oliveira Petkowicz, Federal University of Parana, Curitiba, Parana, Brazil.
Reviewers:
(1) Anonymous, Institute of Experimental Morphology, Bulgaria.
(2) Anonymous, Bowen University,Nigeria.
Complete Peer review History: http://www.sciencedomain.org/review-history.php?iid=652&id=3&aid=6023

Short Research Article

Received 26th July 2014
Accepted 13th August 2014
Published 9th September 2014

ABSTRACT

Aims: The presented research paper is aimed to prevalence of apoptosis for the first time by using *in silico* molecular docking and simulation using caspase-3 zymogen and zinc-coordinated compounds. Antioxidant activities of the coordinated complexes were compared to the positive controls (BHT and ascorbic acid).
Study design: Molecular docking analysis was performed by using Autodock 4.2, setting at 150x140x110 Gridbox, center at -57.616, 31.092, 88.666 with 0.375 Å spacing. Their antioxidant activity was tested by FRAP and DPPH assay.
Place and Duration of Study: Department of Chemistry and department of molecular medicine, Faculty of Medicine, University of Malaya laboratories between January 2014 – July 2014
Methodology: Compounds derived from zinc(II) ion give rise to coordination complexes exhibited CHN, NMR (^{1}H & ^{13}C) and FT-IR spectra consistent with the proposed structures. Based on the x-

**Corresponding author: Email: nura_suleiman@yahoo.com;*

ray crystal structure, one of the derivatives is a mononuclear square-pyramidal metal complex, with τ value of 0.35. The molecular docking simulation formed between compounds and caspase 3 showed the ligands bind to the active-site gorge well positioned in the active-site gorge**.**

Results: The residues that have been involved in this protein-ligand interaction docked well by using Autodock 4.2, setting at 150x140x110 Gridbox, center at -57.616, 31.092, 88.666 with 0.375 Å spacing in the hydrophobic pocket. Their antioxidant activity tested revealed their FRAP assay values of 531.11±0.021 and 1886.11±0.008 higher than value of 187.3±2.6 shown by BHT used as standard. The compounds showed IC_{50} values 21.50±0.009 and 14.80±0.002 lower than ascorbic acid with an IC_{50} value of 2.26±0.001 µg/mL.

Conclusion: Synthesized zinc(II) complexes have been confirmed to inhibit the activity of caspase 3 both *in silico* and *in vitro* and were tested for antioxidant activity by both FRAP and DPPH methods.

Keywords: Caspase 3; Zinc(II)complexes; docking; antioxidant; x-ray crystallography.

ABBREVIATIONS

BHT= Butylated hydroxytoluene; FRAP = Ferric Reducing Antioxidant Power; DPPH = 1,1-diphenyl-2-picryl-hydrazyl; CHN = Carbon, Hydrogen and Nitrogen; NMR = Nuclear Magnetic Resonance

1. INTRODUCTION

Caspases are cysteine proteases that cleave their substrate protein specifically behind an aspartate residue (review in [1]). They are normally present as inactive pro-enzymes. Caspases exist as inactive pro-enzymes able to undergo proteolytic processing at conserved aspartic residues to produce two subunits, large and small, that dimerize to form the active enzyme. For the full enzymatic activity of caspases, they require cleavage at specific internal aspartate residues, which separate large and small subunits from each other [1].

In cancer, the apoptosis induction without caspase activity may produce new pharmacological targets for treatment of cancer disease. Therefore, it is worthwhile to identify the mechanisms of apoptosis in the absence of caspase activity. For example, in exhibition of caspase-dependent apoptosis in the normal cell, in cancer cells a death by caspase-independent apoptosis is possible during protection of normal tissues by caspase inhibitors [2] Caspase activation according to genetic and biochemical studies is essential for the occurrence of the apoptotic phenotype of cell death [3]. However, apoptosis is not always dependent on caspases, because cells can die through a non-apoptotic morphology even when caspase activity is inhibited [4,5,6]. Caspase inhibitors have been shown to prevent cardiomyocyte death in response to simulated ischemia in vitro [7] and in ischemic–reperfused myocardium together with reduction of myocardial infarct size [8,9].

Caspase-3 is a protein encoded by the *CASP3* gene. *CASP3* orthologs [10] have been identified in numerous mammals as complete genome data available. It is also a member of the cysteine-aspartic acid protease family [11]. The catalytic site of caspase-3 involves the sulfohydryl group of Cys-285 and the imidazole ring of His-237. His-237 stabilizes the carbonyl group of the key aspartate residue, while Cys-285 attacks the peptide bond during its cleavage. Cys-285 and Gly-238 also function to stabilize the tetrahedral transition state of the substrate-enzyme complex through hydrogen bonding [12]. In vitro, caspase-3 has been found to prefer the peptide sequence DEVDG (Asp-Glu-Val-Asp-Gly) with cleavage occurring on the carboxy side of the second aspartic acid residue (between D and G).[13,12,14] Caspase-3 is active over a broad pH range that is slightly higher (more basic) than many of the other executioner caspases. This broad range indicates that caspase-3 would be fully active in normal and apoptotic cell conditions [15]. Caspase-3 inhibition is by means of XIAP that binds and suppresses the action of caspase-9, which is directly involved in the activation of executioner caspase-3 [16]. During the caspase cascade, however, caspase-3 functions to inhibit XIAP activity by cleavage of caspase-9 at a specific site, preventing in this way XIAP from being able to bind to inhibit caspase-9 activity [17].

Zinc is the second most prominent trace metal in the human body after iron. While deficiency of zinc may cause growth effects, few noxious effects of excess zinc have been observed and zinc is one of the metals with the lowest toxicity.

It is involved in a large number of enzymatic functions; fulfilling both structural and catalytic roles [18]. These functions include CT-DNA binding mononucleotides and cleavage activity [19], therapeutic agents [20], antibacterial and cytotoxic activities [21], DNA binding, antioxidant and antibacterial activities [22], DNA binding, photonuclease activity and in vitro antimicrobial effectiveness [23], DNA binding ability, chemical nuclease activity and antimicrobial evaluation [24]. Zinc-containing proteins have recently been proved as attractive targets for chemotherapy.

Zinc is a regulator of caspase-3, also reported as antioxidant, microtubule stabilizer, growth co-factor, and anti-inflammatory agent [25]. It is one of the most widely distributed biometals found in living tissues [26] Zn is a cellular regulator of caspase-3 activation and it is also co-localized with the zymogen form of caspase-3 in the apical cytoplasm of sheep and human airway epithelial cells [27]. The protective effect of Zn^{2+} has been attributed to its inhibition of a Ca^{2+}- and Mg^{2+}-dependent endonuclease [28], thereby causing inhibition of DNA fragmentation, a terminal step and hallmark of apoptosis. However, the concentrations of Zn^{2+} used for inhibition of the purified Ca^{2+}-dependent endonuclease were in the millimolar range [29]. Furthermore, Zn^{2+} has been found to inhibited both TNF-a- and etoposide-induced cytotoxicity, as assessed by methylene blue staining, prior to effects on DNA fragmentation [30]. Zn^{2+} has also been demonstrated to suppress the protease responsible for cleavage of lamins in cell-free extracts [31]. Moreover, Zn^{2+} has been characterized as a potent inhibitor of caspase-3-containing apoptotic extract and by purified recombinant caspase-3. Therefore, caspase-3 is a novel and proximal site of Zn^{2+} inhibition in the apoptotic pathway.

The main goal of the current research manuscript is connected with the reveal of apoptosis by caspase inhibitors in the absence of caspase activity for the first time by using *in silico* molecular docking and simulation using caspase-3 zymogen and zinc-coordiated compounds. In addition, the antioxidant activities of the coordinated complexes were tested and their IC_{50} values were compared to the positive control (ascorbic acid).

2. EXPERIMENTAL DETAILS

Physical measurements: Melting points were determined using a Perkin–Elmer DSC 6 (Differential Scanning Calorimeter) instrument. The IR spectra were recorded on a Perkin–Elmer RX1 FT IR spectrometer with pure samples prepared. All the spectra were run in the range 400–4000 cm^{-1} at room temperature. The ^1H NMR spectra were recorded in DMSO-d_6 on a Lambda JEOL 400 MHz FT-NMR spectrometer. The electronic spectra were measured by means of a Shimadzu 1601 spectrophotometer in the region 200–1100 nm.

Chemicals and reagents: 4-(2-aminoethyl)morpholine and 2-acetylpyridine were purchased from the Aldrich–Sigma Company. Ethanol was distilled prior to use. All chemicals were of analytical grades and used without any further purification.

2.1 General method for complex Preparation

.

All the complexes were obtained by *in situ* method as reported by [Suleiman *et. al.* 2012]. The metal salts were added directly prior to the isolation of ligand. Dibromido {2-morpholino-*N*-[1-(2-pyridyl) ethylidene] ethanamine-K^3N,N',N''}zinc [$Zn(LMA)Br_2$] was synthesized according to [32]. The product was dried in a vacuum desiccator. The x-ray crystal structure of the zinc (II) complex was previously published [33]. The second compound Diazido{2-morpholino-N-[1-(2-pyridyl) ethylidene] ethanamine-K^3N,N',N''}zinc [$Zn(LMA)(N_3)_2$] was synthesized by reacting 2-acetylpyridine (0.20 g, 1.65 mmol) and 4-(2-aminoethyl)morpholine (0.21 g, 1.65 mmol) in ethanol (20 ml) was refluxed for 2 hr followed by addition of a solution of zinc(II) acetate dihydrate (0.36 g, 1.65 mmol) and sodium azide (0.22 g, 3.30 mmol) in a minimum amount of water. The resulting solution was refluxed for 30 min, and then left at room temperature. The crystals of the title complex were obtained in a few days; the resulting pure crystal was filtered off, washed with cold ethanol and dried over silica gel. Melting point 228.78 ºC; Anal. Calc. for [$Zn(C_{13}H_{19}N_3O)(N_3)_2$] C, 40.80; H, 5.00; N, 32.94; Found C, 40.88; H, 5.10; N, 32.98; IR (ATR cm−1): 2874, 2839w ν(C-H), 2070, 2043 ν(N_3), 1654 ν(C=N), 1433m ν(C-C), 1118m ν(C-N), 566 ν(M-N). UV-Vis [λ_{max} (nm) (DMSO)]: 492 (LMCT), 409 (n→π*); 224 (π→π*). ^{1}H-NMR (DMSO-d^6),ppm: 8.688, 8.680 [d, 1H, δ(Ar-H)pyr], 8.363, 8.350, 8.307, 8.294 [m, 2H, δ(Ar-H)pyr], 7.933, 7.925, 7.913 [d, 1H, δ(Ar-H)pyr], 3.693, 3.685, 3.678 [m, 6H, δ(3N-CH2)], 2.760, 2.750, 2.740 [t, 2H, δ($2CH_2$)], 2.624 [s, 3H, δ(CH_3)], 2.513 [s, 2H, δ(CH_2=)].

^{13}C-NMR (DMSO-d^{6}),ppm: 169.11 [1C, δ(C=N)], 148.63 δ(C), 140.69 δ(CH), 137.47 δ(CH), 127.81 δ(CH), 124.52 δ(CH) [5C, δ(Ar-pyr)], 63.90 [2C, δ($2CH_2$)], 57.30, 53.42, [2C, δ($2CH_2$)], 53.11, [1C, δ(CH_2)], 15.86, [1C, δ(CH_2)], 44.07 [1C, δ(CH_3)],

2.2 Single Crystal X-Ray Diffraction

Diffraction data were measured using a Bruker SMART Apex II CCD area-detector diffractometer (graphite-monochromated Mo K radiation, = 0.71073 Å). The orientation matrix, unit cell refinement and data reduction were all handled by the Apex2 software (SAINT integration, SADABS absorption correction) [34]. The structure was solved using direct method in the program SHELXS-97 [35] and was refined by the full matrix least-squares method on *F2* with SHELXL-97. All the non-hydrogen atoms were refined anisotropically and all the hydrogen atoms were placed at calculated positions and refined isotropically. Drawing of the molecule was produced with XSEED [36]. Crystal data and refinement are summarized in Table 1.

2.3 Molecular Modeling Evaluations

The enzyme coordinates were deposited in the Protein Data Bank for caspase-3 (1PAU) after eliminating the inhibitor (AC-DEVD-CHO) and water molecules. The missing residues were built and polar hydrogen atoms were added using Discovery Studio 3.0 program (Accelrys, Inc., San Diego, CA, USA). By default, solvation parameters and Kollman charges were assigned to all atoms of the enzyme using AutoDock Tools v.1.4. The 3D structures of the compounds were optimized according to the standard protocol in Discovery Studio 3.0. For docking studies, the latest version of AutoDock v.4.0 [37] was chosen because its algorithm allows full flexibility of small compounds. It has been shown to successfully reproduce many crystal structure complexes and includes an empirical binding free energy evaluation. Docking of compounds to caspase-3 was carried out using the hybrid Lamarckian Genetic Algorithm. A grid box with the size of 150 x 140 x 110 points along the xyz axes, and grid spacing of 0.375 Å was built to span the entire protein structure, *in vacuo*. The maximum number of energy evaluations was set to 25,000,000. Blind docking was used to predict structural features of compound binding. Resulting docked orientations within a root-mean square deviation of 1.5 Å were clustered. The lowest energy cluster reported by AutoDock for the compound was used for further analysis. All other parameters were maintained at their default settings. The structure of the complex obtained was visualized and analyzed using Discovery Studio Visualizer 3.0.

Table 1. Crystal data and structure refinement for Zn(LMA)$(N_3)_2$ complex

Identification code	[Zn(LMA)$(N_3)_2$]
Empirical formula	$C_{13}H_{19}N_9OZn$
Formula weight	382.74
Temperature/K	373(2)
Crystal system	monoclinic
Space group	$P2_1/c$
a/Å	10.7118(19)
b/Å	9.2241(16)
c/Å	17.110(3)
α/°	90.00
β/°	105.719(2)
γ/°	90.00
Volume/Å^3	1627.4(5)
Z	4
ρ_{calc}mg/mm^3	1.562
m/mm^{-1}	1.531
F(000)	792.0
Crystal size/mm^3	0.25 × 0.06 × 0.05
2Θ range for data collection	4.94 to 52.82°
Index ranges	-13 ≤ h ≤ 13, -11 ≤ k ≤ 11, -21 ≤ l ≤ 18
Reflections collected	8625
Independent reflections	3323[R(int) = 0.0582]
Data/restraints/parameters	3323/0/218
Goodness-of-fit on F^2	1.011
Final R indexes [I>=2σ (I)]	R_1 = 0.0459, wR_2 = 0.0870
Final R indexes [all data]	$C_{13}H_{19}N_9OZn$
Largest diff. peak/hole/e Å^{-3}	382.74

2.4 Antioxidant Activity

FRAP Assay: The FRAP assay of the compounds performed using modified method as described by Benzie and Strain [38]. The stock solutions contained 300 mM acetate buffer (3.1 g $C_2H_3NaO_2 \cdot 3H_2O$ and 16 mL C_2H_4O2), pH 3.6, 10 mM TPTZ (2,4,6-tripyridyl-*s*-triazine) solution in 40 mM hydrochloric acid and 20 mM ferric chloride hexahydrate solution. The fresh working solution was prepared by mixing acetate buffer (25 mL), TPTZ (2.5 mL), and ferric chloride hexahydrate solution (2.5 mL). The temperature of the solution was raised to 37 ℃ before use and allowed to react with the FRAP solution (300 µL) on a dark. The colored product (ferrous tripyridyltriazine complex) was monitored at a wavelength of 593 nm. The standard curve was linear between 100 and 1,000 µM ferrous sulphate. Results are expressed in µM ferrous/g

dry mass and compared with that of ascorbic acid and butylatedhydroxytoluene.

DPPH (1,1-Diphenyl-2-picrylhydrazyl) Assay: The scavenging activities of the compounds on DPPH were recorded according to a reported procedure [39]. The compounds showed final concentrations within the range of 0–25 µg/mL in methanol. One milliliter of 0.3 mM DPPH ethanol solution was added to sample solution (2.5 mL) of different concentrations and used as stock solutions for the test; meanwhile methanol (1 mL) was added to samples (2.5 mL) to make the blank solutions. The negative control (blank) consisted of DPPH solution (1 mL) plus methanol (2.5 mL). These solutions were allowed to react at room temperature for 30 min on a dark. The absorbance was read at 518 nm and converted into percentage antioxidant activity according to the following equation: % Inhibition = [(AB − AA)/AB] × 100. Where: AB: absorption of blank sample, AA: absorption of tested samples. The kinetics of DPPH scavenging activity was determined and the IC_{50} calculated using ascorbic acid as a positive control.

3. RESULTS AND DISCUSSION

The *N,N',N"* donor Schiff base ligand coordinates zinc(II) ion gives a rise to coordination complexes (Scheme 1). The compounds exhibited CHN, NMR (^{1}H & ^{13}C) and FT-IR spectra were consistent with the proposed structures which allowed the synthesized complexes to be recognized as *Diazido{2-morpholino-N-[1-(2-pyridyl) ethylidene]ethanamine-κ^3N,N',N"}zinc* [Zn(LMA)$(N_3)_2$] and *Dibromido {2-morpholino-N-[1-(2-pyridyl) ethylidene] ethanamine-K^3N, N', N"} zinc* [Zn(LMA)Br_2] (Scheme 1). Complexes possessed elongated geometry with the two weakly coordinating acetate ions where by the Br^- and N_3^- ions when added to the solution, replaces the acetate ions due to its stronger coordinating ability (Scheme 1). In this context we compare the structures of some earlier prepared complexes with those of the presented substances. Two reported complexes of nickel(II) perchlorate were revealed, with the similar donor-Schiff base only different of piperidine instead of morpholine amine substituent [40].

3.1 Fourier Transformed-Infrared Spectra (FT-IR)

The IR spectra of transition metal complexes were carried out at 4000–400 cm^{-1} range. The characteristic IR stretching frequencies of the metal complexes along with their proposed assignments are summarized in the experimental part. There are similarities in the IR spectrum of the metal complexes to each other, except of some slight variations in the shifts and intensities of few vibration peaks caused by different metal(II) ions, indicating that the metal complexes have similar structure to each other. However, some significant differences between the structure of zinc(II)bromide complex and that of zinc(II)azide complex were also revealed, as expected.

The IR spectra of all the complexes possess very strong characteristic absorption bands in the region of 1649 – 1661cm^{-1} which is attributed to the C=N stretching vibration of the Schiff base imino functional group [41-45]. For Zn(LMA)$(N_3)_2$ this specter was observed at a region of 2070 and 2043 which is attributed to zinc in the azide metal bond [46]. All the spectra for the complexes show M – N bands at a lower wavelength in the range of 477 – 575 cm^{-1} [47-50].

3.2 Ultraviolet – Vis Spectral Analysis (UV-Vis)

The electronic spectra of all complexes were obtained in DMSO solvent and showed absorption bands in three distinct regions. The first region ranging from 224 to approximately 280 nm, is characteristic for the electronic inter – ligand π→π* transitions [51], while the second characteristic wavelength in the region of 281 nm to approximately 409 nm is the second inter ligand n→π transition [52]. The third distinct region ranging from 492 nm to approximately 606 nm is the characteristic for the ligand to metal charge transfer (LMCT) from the nitrogen atom to the transition metal centre [53].

3.3 ^{1}H-NMR and ^{13}C-NMR – Spectra

Chemical shifts in the regions 7.89 - 8.78 ppm and 7.91 – 8.69 were observed for Zn(LMA)Br_2 and (Zn(LMA)$(N_3)_2$ respectively and they were assigned to the aromatic ring protons [54]. The other single peaks appeared in the region 2.62 ppm and 2.62ppm respectively were attributed to δ(CH_3) indicating the methyl on the carbonyl group in zinc complexes [54].

In the ^{13}C NMR spectra of the metal complexes, the signal at 168.38 ppm and 169.11 can be assigned to the azomethine carbon atoms for Zn(LMA)Br_2 and (Zn(LMA)$(N_3)_2$ complexes, respectively [54]. Similarly, aromatic ring carbon

atoms of the ligands were determined in the 124.05 –148.43ppm and 121.12 – 148.63 ppm range, respectively [49].

3.4 X-ray Crystallography

The compound tested is a square-pyramidal zinc(II) complex in which the metal center is coordinated by the *N,N',N"*-tridentate Schiff base and the *N* atoms of two azide ligands (Fig. 1). The $CH_2N(CH_3)_2$ fragment is disordered over two sets of sites in a 0.53(4):0.471 (4) ratio. Like the structure of the zinc(II) thiocyanate complexes of similar Schiff bases [55,56], the presented structure is a mononuclear square-pyramidal metal complex, with the τ-value 0.35. In the crystal structure of the title compound, C---H...N interactions connect a pair of molecules, related by symmetry −x+1, −y, −z, around a center of inversion. The zinc atom is bonded to three donor nitrogen atoms of the ligand and two azides coordinated through the nitrogen atoms ending.

3.5 Molecular Docking

The crystal structure of caspase 3 protein (pdb id: 1PAU) is a member of the **c**ysteine-aspartic acid protease (caspase) family [57] Sequential activation of caspase 3 plays a central role in the execution-phase of cell apoptosis. The catalytic site of caspase-3 involves the sulfohydryl group of Cys-285 and the imidazole ring of His-237. His-237 stabilizes the carbonyl group of the key aspartate residue, while Cys-285 attacks to ultimately cleave the peptide bond. Cys-285 and Gly-238 also function to stabilize the tetrahedral transition state of the substrate-enzyme complex through hydrogen bonding [58].

3.5.1 Molecular docking of caspase-3 with $Zn(LMA)(N_3)_2$ complex

The residues that were found to be involved in this protein-ligand interaction of $Zn(LMA)(N_3)_2$ docked well by using Autodock 4.2, setting at 150x140x110 Gridbox, center at -57.616, 31.092, 88.666 with 0.375 Å spacing in the hydrophobic pocket of GLN283, CYS285, SER236, HIS237, THR177, SER178, ARG179, TYR338, SER339, TRP340 and ARG341. Two Pi – Cation Interaction between Ligand Benzene Ring and Ammonium ion (NH^+) of ARG179, and Benzene ring of TRP340 and N atom of the Ligand. The molecular docking simulation of the complex formed between compounds and caspase 3 (Fig. 2) showed the ligand bind to the active-site gorge as well positioned in this place (Fig. 2).

A closer inspection of the interactions (Fig. 2) indicated the presence of five inter-molecular hydrogen bonding, LIGAND:N21 - SER339:O, LIGAND:N24 - THR177:O, LIGAND:N24 - THR177:OG1, LIGAND:N24 - SER178:O, LIGAND:N24 - HIS237:NE2 with a distance of 2.94064, 2.81524,3.10411,2.93221 and 3.10764, respectively (Table 2). A hydrogen 229 bond between GLN283:NE2 and SER339:O with a distance of 3.0722 Å was also observed.

3.5.2 Molecular docking of caspase-3 with $Zn(LMA)Br_2$ complex

The residues that were proved to be involved in the protein-ligand interaction of $Zn(LMA)Br_2$ docked well in the hydrophobic pocket of GLN283, ALA284, CYS285, SER236, HIS237, THR177, ARG179, TYR338, SER339, TRP340, and ARG341. The molecular docking simulation of the complex formed between compounds and caspase 3 (Fig. 3) showed the ligand bind to the active-site gorge well positioned in the active-site gorge. One Pi – Cation Interaction between Ligand Benzene Ring and Ammonium ion (NH^+) of ARG179 was observed.

A closer inspection of the interactions (Fig. 3) indicated an inter-molecular hydrogen bonding between Ligand: Br and ARG341:N with the distance: 3.1785 Å, and another hydrogen bond between GLN283:NE2 and SER339:O with the distance : 3.0722 Å.

3.6 Roles of Caspase-3 in Complex-induced Apoptosis

For further confirmation of the inhibition of caspase-3 activity by zinc complex, potential molecular mechanisms involved, colorimetric was upon treatment with 1.5, 3 and 4.5 µg/ml zinc complex for 48 h. The activity of caspase-3 does not show any significant changes after administration of zinc complexes via the intrinsic mitochondrial apoptotic pathway in caspase-3 activity, which confirmed the inhibition of caspase-3 activity by zinc complexes.

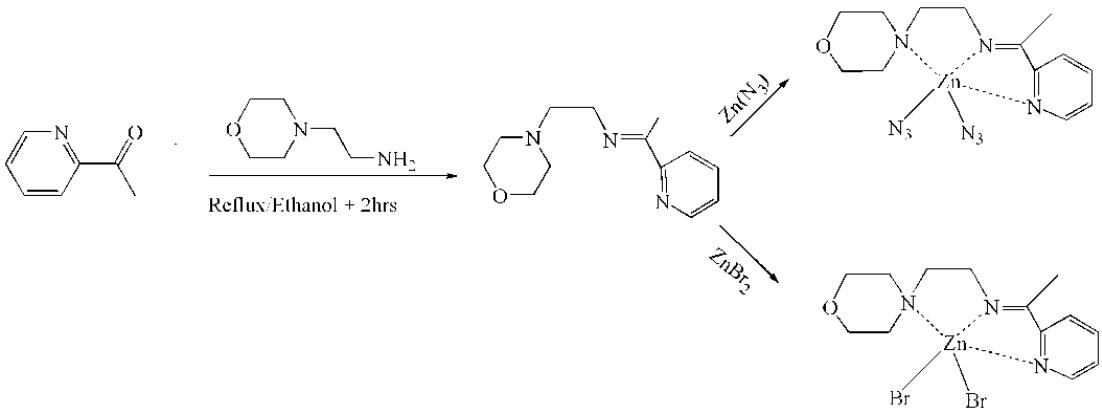

Scheme 1. Molecular structures of the zinc(II) ion complexes

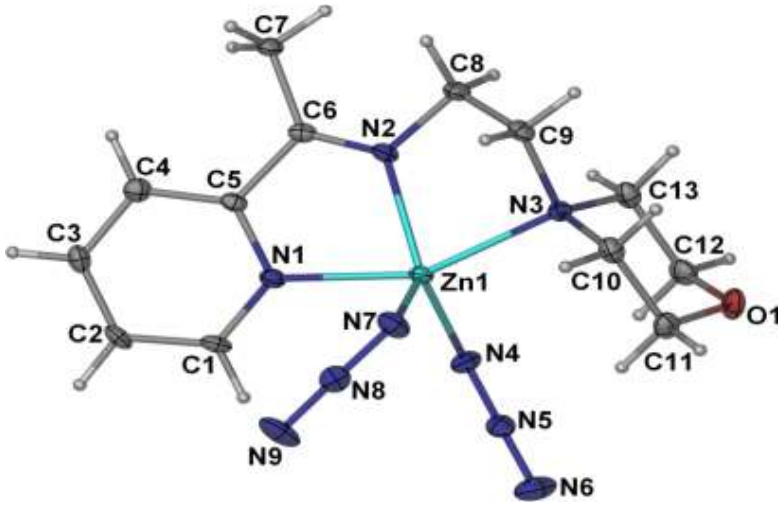

Fig. 1. Crystal structure for $[Zn(N_3)_2(C_{13}H_{19}N_3O)]$

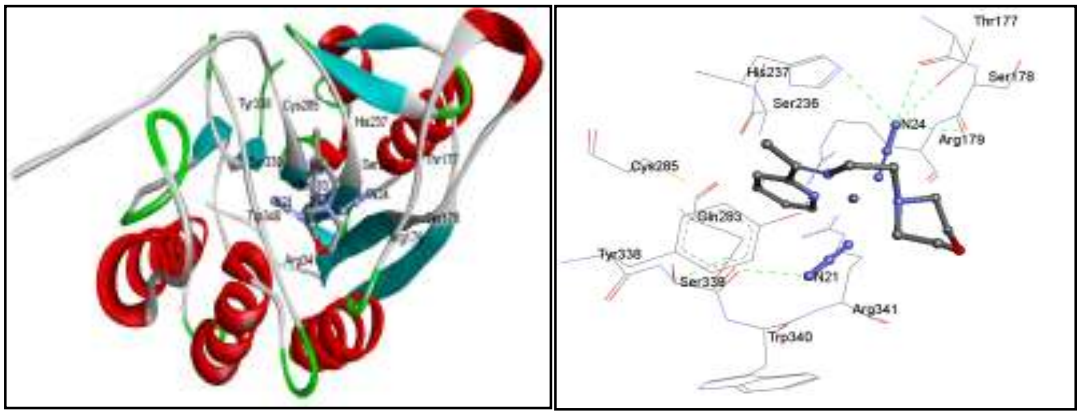

Fig. 2. Representations of the molecular model of the complex formed between Zn(LMA)$(N_3)_2$ and caspase 3 zymogen, and 3D representation of the ligand-enzyme binding interactions, respectively. Zn(LMA)$(N_3)_2$ Compound is represented as a dark grey sticks, and the hydrogen bonds – as green dashed lines

Table 2. Hydrogen bond interactions between $Zn(LMA)(N_3)_2$ and hAChE

	Distance(Å)	Donor Atom	Acceptor Atom
LIGAND:N21 - SER339:O	2.94064	N21	O
LIGAND:N24 - THR177:O	2.81524	N24	O
LIGAND:N24 - THR177:OG1	3.10411	N24	OG1
LIGAND:N24 - SER178:O	2.93221	N24	O
LIGAND:N24 - HIS237:NE2	3.10764	N24	NE2

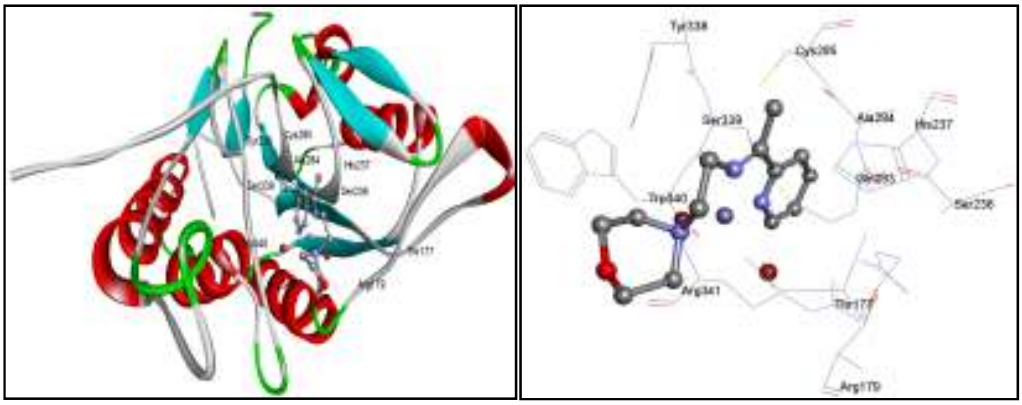

Fig. 3. Representations of the molecular model of the complex formed between $Zn(LMA)Br_2$ and caspase 3 zymogen, and 3D representation of the ligand-enzyme binding interactions. $Zn(LMA)Br_2$ Compound is represented as a dark-grey sticks, and hydrogen bonds – as green dashed lines

3.7 Antioxidant Assays

The antioxidant activities of the complexes $Zn(LMA)Br_2$ and $(Zn(LMA)(N_3)_2$ were tested. For this goal, the color change from deep purple to yellow at 515 nm observed in the DPPH assay has confirmed the radical scavenging activity of the compounds. A reference curve of absorbance (A) against DPPH concentration in methanol was plotted and used for the calculation of DPPH concentration at various reaction times (R^2 = 0.99). The compounds show IC_{50} values 21.50±0.009 and 14.80±0.002 corresponding to $Zn(LMA)Br_2$ and $(Zn(LMA)(N_3)_2$ respectively among the series (Table 3). All the compounds tested IC_{50} were compared to the positive control used (ascorbic acid) with an IC_{50} value of 2.26±0.001 µg/mL.

The second method used for testing the antioxidant activities of these compounds was the FRAP assay. It is considered as an accurate method for assessing "antioxidant power". Ferric to ferrous ion reduction at low pH causes a colored ferrous-tripyridyltriazine complex to form. FRAP values are obtained by comparing the absorbance change at 593 nm in test reaction mixtures with those containing ferrous ions at known concentrations. In this study, the compounds $Zn(LMA)Br_2$ and $(Zn(LMA)(N_3)_2$ showed in FRAP assay, the highest values can be 531.11±0.021 and 1886.11±0.008 respectively (Table 3) which is above the value of 187.3±2.6 shown by BHT used as standard. It was observed that highest in FRAP assay this can be attributed to increased in π-electron delocalization within the pyridine ring which increases the electron density and causes ferric ion change to ferrous [59].

Table 3. Anti-oxidant activities of the tested compounds

Compounds	Molecular weight	DPPH (IC_{50}, µg/mL)	FRAP value (Mean ± SD)
1- $Zn(LMA)Br_2$	458.51	21.50±0.009	531.11±0.021
2-$(Zn(LMA)(N_3)_2$	382.74	14.80±0.002	1886.11±0.008
3-Ligand	233.31	18.20±0.007	1580.00±0.016
Ascorbic acid	-	2.26±0.001	19400.00±0.007
BHT	-	NA	187.30±2.600

4. CONCLUSION

New zinc(II) metal complexes of some newly synthesized 4-(2-aminoethyl)morpholine donor Schiff base ligands with 2-acetylpyridine in presence of Br^- and N_3^- ions were confirmed to inhibit the activity of caspase 3 both *in silico* and *in vitro*, and were tested for antioxidant activity by both FRAP and DPPH methods.

COMPETING INTERESTS

Authors have declared that no competing interests exist.

REFERENCES

1. Thornberry NA, Lazebnik Y. Caspases: enemies within. Science 1998;281:1312–1316.
2. Brian SC, Gilbert RK, Laura JCB, Rick GS. Identification of caspase-independent apoptosis in epithelial and cancer cells. The Journal of Pharmacology and Experimental therapeutics. JPET. 2004;310(1):126–134.
3. Hirsch T, Marchetti P, Susin SA. The apoptosis–necrosis paradox. Apoptogenic proteases activated after mitochondrial per meability transition determine the mode of cell death. Oncogene. 1997;15:1573–1581.
4. McCarthy NJ, Whyte MKB, Gilbert CS, Evan GI. Inhibition of Ced-3/ ICE-related proteases does not prevent cell death induced by oncogenes, DNA damage, or the Bcl-2 homologue Bak. J Cell Biol. 1997;136:215–227.
5. Brunet CL, Gunby RH, Benson RS, Hickman JA, Watson AJ, Brady G. Commitment to cell death measured by loss of clonogenicity is separable from the appearance of apoptotic markers. Cell Death Different. 1998;5:107–115.
6. Amarente-Mendes GP, Finucance DM, Martin SJ, Cotter TG, Salvesen GS, Green DR. Anti-apoptotic oncogenes prevent caspase dependent and independent commitment for cell death. Cell Death Different. 1998;5:298–306
7. Gottlieb RA, Gruol DL, Zhu JY, Engler RL. Preconditioning in rabbit cardiomyocytes. Role of pH, vacuolar proton ATPase, and apoptosis. J Clin Invest 1996;97:2391–2398.
8. Holly TA, Drincic A, Byun Y, et al. Caspase inhibition reduces myocyte cell death induced by myocardial ischemia and reperfusion in vivo. J Mol Cell Cardiol. 1999;31:1709–1715.
9. Yaoita H, Oqawa K, Maehara K, Maruyama Y. Attenuation of ischemia / reperfusion injury in rats by a caspase inhibitor. Circulation. 1998;97:276–281.
10. "OrthoMaM phylogenetic marker: CASP3 coding sequence".
11. Alnemri ES, Livingston DJ, Nicholson DW, Salvesen G, Thornberry NA, Wong WW, Yuan J. Human ICE/CED-3 protease nomenclature. Cell. 1996;87(2):171. doi:10.1016/S0092-8674(00)81334-3. PMID 8861900.
12. Lavrik IN, Golks A, Krammer PH. Caspases: Pharmacological manipulation of cell death". J. Clin. Invest. 2005;115(10):2665–72. doi:10.1172/JCI26252. PMC 1236692. PMID 16200200.
13. Stennicke HR, Renatus M, Meldal M, Salvesen GS. “Internally quenched fluorescent peptide substrates disclose the subsite preferences of human caspases 1, 3, 6, 7 and 8". Biochem. J. 2000;350. Pt 2:563–8. PMC 1221285. PMID 10947972.
14. Porter AG, Jänicke RU. Emerging roles of caspase-3 in apoptosis. Cell Death Differ. 1999;6(2):99–104. doi:10.1038/sj.cdd.4400476. PMID 10200555.
15. Stennicke HR, Salvesen GS. Biochemical characteristics of caspases-3, -6, -7, and -8. J. Biol. Chem. 1997;272(41):25719–23. doi:10.1074/jbc.272.41.25719. PMID 9325297.
16. Li P, Nijhawan D, Wang X. Mitochondrial activation of apoptosis. Cell 2004;116(2):S57–9,2,S59. doi:10.1016/S0092-8674(04)00031-5. PMID 15055583.
17. Lavrik IN, Golks A, Krammer PH. "Caspases: Pharmacological manipulation of cell death". J. Clin. Invest. 2005;115(10):2665–72. doi:10.1172/JCI26252. PMC 1236692. PMID 16200200.
18. Powis G, Hacker MP. The toxicity of anticancer drugs. Pergamon Press: New York, USA. 1991;106.
19. Arjmand, F, Sayeed F. Synthesis of new chiral heterocyclic Schiff base modulated Cu(II)/Zn(II) complexes: Their comparative binding studies with CT-DNA,

mononucleotides and cleavage activity. J. Photochem. Photobiol. 2011;103:66-179.
20. Creaven BS, Devereux M. Quinolin-2(1H)-one-triazole derived Schiff bases and their Cu(II) and Zn(II) complexes: Possible new therapeutic agents. Polyhedron. 2010;29:813-822.
21. El-Sherif AA, Eldebss TMA. Synthesis, spectral characterization, solution equilibria, in vitro antibacterial and cytotoxic activities of Cu(II), Ni(II), Mn(II), Co(II) and Zn(II) complexes with Schiff base derived from 5-bromosalicylaldehyde and 2-aminomethylthiophene. Spectrochim. Acta. 2011;79:1803-1814.
22. Khan N-uH, Pandya N. Chiral discrimination asserted by enantiomers of Ni (II), Cu (II) and Zn (II) Schiff base complexes in DNA binding, antioxidant and antibacterial activities. Spectrochim. Acta. 2011;81:199-208.
23. Raman N, Selvan A. Metallation of ethylenediamine based Schiff base with biologically active Cu(II), Ni(II) and Zn(II) ions: Synthesis, spectroscopic characterization, electrochemical behaviour, DNA binding, photonuclease activity and in vitro antimicrobial efficacy. Spectrochim. Acta. 2011;79:873-883.
24. Raman N, Sobha Mitu LS. Design, synthesis, DNA binding ability, chemical nuclease activity and antimicrobial evaluation of Cu(II), Co(II), Ni(II) and Zn(II) metal complexes containing tridentate Schiff base. J. Saud. Chem. Soc. in press ; 2011.
25. Vallee BL, Falchuk KH. The biochemical basis of zinc physiology. Physiol. Rev. 1993;73:79–118.
26. Vallee BL. Zinc: Biochemistry, physiology, toxicology and clinical pathology. Biofactors 1988;1:31–36.
27. Truong-Tran AQ, Ruffin RE, Zalewski PD. The role of zinc in caspase activation and apoptotic cell death. Biometals 2001;14:315–330.
28. Cohen JJ, Duke RC. Glucocortocoid activation of a calcium-dependent endonuclease in thymocyte nuclei of leads to cell death J. Immunol. 1984;132:38–42.
29. Gaido ML, Cidlowski JA. Identification, purification, and characterization of a calcium-dependent endonuclease (NUC18) from apoptotic rat thymocytes: NUC18 is not histone H2B. J. Biol. Chem. 1991;266:18580–18585.
30. Fady C, Gardner A, Jacoby F, Briskin K, Tu Y, Schmid I, Lichenstein A. Atypical apoptotic cell death induced in L929 targets by exposure to tumor necrosis factor. J. Interferon Cytokine Res. 1995;15;71–80
31. Takahashi A, Alnemri ES, Lazebnik YA, Fernandes-Alnemri T, Litwack G, Moir RD, Goldman RD, Poirier GG, Kaufmann SH, Earnshaw WC. Cleavage of lamin A by Mch2a but not CPP32: Multiple interleukin 1B-converting enzyme-related protease with distinct substrate recognition properties are active in apoptosis Proc. Natl. Acad. Sci. U. S. A. 1996;93:8395–8400
32. Gwaram NS, Ali HM, Khaledi H, Abdulla MA, Hadi AH, et al. Antibacterial evaluation of some Schiff bases derived from 2-acetylpyridine and their metal complexes. Molecules 2012;17:5952–5971.
33. Ding YW, Wang XL, Ni LL. Dibromido{2-morpholino-N-[1-(2-pyridyl) ethyl-idene]ethanamine-kappaN,N',N''}zinc (II). Acta Crystallogr Sect E Struct Rep Online 2011;67: m261.
34. Bruker APEX2 and SAINT. Bruker AXS Inc.: Madison, WI, USA; 2007.
35. Sheldrick GM. A short history of SHELX. Acta Crystallogr. A 2008;64:112–122.
36. Barbour, LJ. X-Seed-A software tool for supramolecular crystallography. J. Supramol. Chem. 2001;1:189–191.
37. Morris GM, Goodsell DS, Halliday RS, Huey R, Hart WE, Belew RK, Olson AJ. Automated docking using a Lamarckian genetic algorithm and empirical binding free energy function. J. Comput. Chem. 1998;19:1639–1662.
38. Suparna B, Biao W, Paul GL, Christoph JAG. Synthesis, structure and bonding of cadmium(II) thiocyanate systems featuring nitrogen based ligands of different denticity. Inorg. Chim. Acta. 2005;358:535–544.
39. Pallab B, Shouvik C, Michael GBD, Carmen D. Ashutosh G. Synthesis, structure and magnetic properties of mono- and di-nuclear nickel(II) thiocyanate complexes with tridentate N3 donor Schiff bases; Polyhedron 2010;29:2637–2642.
40. Inamur RL, Tapas KM, Debasis D, Tian –HL, Wing –TW, Ken-ichi O, Nirmalendu RC. Syntheses, characterisation and solid state thermal studies of 1-(2-aminoethyl)piperidine (L), 1-(2-aminoethyl)pyrrolidine (L) and 4-(2-

aminoethyl)morpholine (L.) complexes of nickel(II): X-ray single crystal structure analyses of trans-[NiL2(CH3CN)2](ClO4)2, trans-[NiL2(NCS)2] and trans-[NiL-2(NCS)2]; Polyhedron. 2001;20:2073–2082.

41. Raman, N, Selvan A. Metallation of ethylenediamine based Schiff base with biologically active Cu(II), Ni(II) and Zn(II) ions: Synthesis, spectroscopic characterization, electrochemical behaviour, DNA binding, photonuclease activity and in vitro antimicrobial efficacy. Spectrochimica Acta Part A: Molecular and Biomolecular Spectroscopy. 2011;79:873-883.
42. Khan N-uH, Pandya N. Chiral discrimination asserted by enantiomers of Ni (II), Cu (II) and Zn (II) Schiff base complexes in DNA binding, antioxidant and antibacterial activities. Spectrochim. Acta. 2011;81:199-208.
43. Nakamoto K. Infrared and Raman spectra of inorganic and coordination compounds; Wiley: New York, USA; 1978.
44. Inamur RL, Tapas KM, Debasis D, Tian –HL, Wing –TW, Ken-ichi O. Nirmalendu RC. Syntheses, characterisation and solid state thermal studies of 1-(2-aminoethyl)piperidine (L), 1-(2-aminoethyl)pyrrolidine (L) and 4-(2-aminoethyl)morpholine (L.) complexes of nickel(II): X-ray single crystal structure analyses of trans-[NiL2(CH3CN)2](ClO4)2, trans-[NiL2(NCS)2] and trans-[NiL-2(NCS)2]; Polyhedron. 2001;20:2073–2082.
45. Suparna B, Biao W, Paul GL, Christoph JAG. Synthesis, structure and bonding of cadmium(II) thiocyanate systems featuring nitrogen based ligands of different denticity. Inorg. Chim. Acta. 2005;358:535–544.
46. Pallab B, Shouvik C, Michael GBD, Carmen D, Ashutosh G. Synthesis, structure and magnetic properties of mono- and di-nuclear nickel(II) thiocyanate complexes with tridentate N3 donor Schiff bases. Polyhedron. 2010;29:2637–2642.
47. Mohamed M, Hapipah MA, Mahmood AA, Robinson TW. Synthesis, structural characterization, and anti-ulcerogenic activity of Schiff base ligands derived from tryptamine and 5-chloro, 5-nitro, 3,5-ditertiarybutyl salicylaldehyde and their nickel(II), copper(II), and zinc(II) complexes. Polyhedron. 2009;28:3993–3998
48. Raman N, Selvan A. Metallation of ethylenediamine based Schiff base with biologically active Cu(II), Ni(II) and Zn(II) ions: Synthesis, spectroscopic characterization, electrochemical behaviour, DNA binding, photonuclease activity and in vitro antimicrobial efficacy. Spectrochim. Acta. 2011;79:873-883.
49. Khan N-uH, Pandya N. Chiral discrimination asserted by enantiomers of Ni (II), Cu (II) and Zn (II) Schiff base complexes in DNA binding, antioxidant and antibacterial activities." Spectrochim. Acta. 2011;81:199-208.
50. Shahabadi N, Kashanian S. DNA binding and DNA cleavage studies of a water soluble cobalt(II) complex containing dinitrogen Schiff base ligand: The effect of metal on the mode of binding. Eur. J. Med. Chem. 2010;45:4239-4245.
51. Chen W, Li Y. Synthesis, molecular docking and biological evaluation of Schiff base transition metal complexes as potential urease inhibitors. Eur. J. Med. Chem. 2010;45:4473-4478.
52. Creaven BS, Duff B. Anticancer and antifungal activity of copper(II) complexes of quinolin-2(1H)-one-derived Schiff bases. Inorg. Chim. Acta. 2010;363:4048-4058.
53. Raman N, Jeyamurugan R. In vivo and in vitro evaluation of highly specific thiolate carrier group copper(II) and zinc(II) complexes on Ehrlich ascites carcinoma tumor model. Eur. J. Med. Chem. 2010;45:5438-5451.
54. Ceyhan G, Çelik C. Antioxidant, electrochemical, thermal, antimicrobial and alkane oxidation properties of tridentate Schiff base ligands and their metal complexes. Spectrochim. Acta. 2011;81:184-198.
55. Cai B-H. [(2-Morpholinoethyl)(2-pyridylmethylene)amine]dithiocyanato zinc(II). Acta. Cryst. 2009;E65, m142.
56. Chen G, Bai Z-P. Qu S-J. [N,N'-Dimethyl-N''-(2-pyridylmethylene) ethane-1,2-diamine] dithiocyanatozinc(II). Acta Cryst. 2005;E61:m2483-m2484.
57. Alnemri ES, Livingston DJ, Nicholson DW, Salvesen G, Thornberry NA, Wong WW, Yuan J. Human ICE/CED-3 protease nomenclature. Cell. 1996;87(2):171. doi:10.1016/S0092-8674(00)81334-3. PMID 8861900.

58. Lavrik IN, Golks A, Krammer PH. "Caspases: Pharmacological manipulation of cell death". J. Clin. Invest. 2005;115(10):2665–72. doi:10.1172/JCI26252.PMC 1236692. PMID 16200200.

59. Stockdale M, Selwyn MJ. Effects of ring substituents on the activity of phenols as inhibitors and uncouplers of mitochondrial respiration. Eur. J. Biochem. 1971;21:565-574.

Peer-review history:
The peer review history for this paper can be accessed here:
http://www.sciencedomain.org/review-history.php?iid= 652&id=3&aid=6023